SLAC-PUB-14105 UCLA/10/TEP/104 MIT-CTP 4150 SB/F/380-10
IPPP/10/34 Saclay IPhT–T10/??? NIKHEF-2010-??? CERN-PH-TH/2010-???

Vector Boson + Jets with BlackHat and Sherpa

C. F. Berger[a], Z. Bern[b], L. J. Dixon[c], F. Febres Cordero[d], D. Forde[ef], T. Gleisberg[c], H. Ita[b], D. A. Kosower[g], D. Maître[h*]

[a]Center for Theoretical Physics, Massachusetts Institute of Technology, Cambridge, MA 02139, USA

[b]Department of Physics and Astronomy, UCLA, Los Angeles, CA 90095-1547, USA

[c]SLAC National Accelerator Laboratory, Stanford University, Stanford, CA 94309, USA

[d]Universidad Simón Bolívar, Departamento de Física, Caracas 1080A, Venezuela

[e]Theory Division, Physics Department, CERN, CH–1211 Geneva 23, Switzerland

[f]NIKHEF Theory Group, Science Park 105, NL–1098 XG Amsterdam, The Netherlands

[g]Institut de Physique Théorique, CEA–Saclay, F–91191 Gif-sur-Yvette cedex, France

[h]Department of Physics, University of Durham, DH1 3LE, UK

We review recent NLO QCD results for W, Z+3-jet production at hadron colliders, computing using BlackHat and SHERPA, and including also some new results for Z + 3-jet production for the LHC at 7 TeV. We report new progress towards the NLO cross section for W + 4-jet production. In particular, we show that the virtual matrix elements produced by BlackHat are numerically stable. We also show that with an improved integrator and tree-level matrix elements from BlackHat, SHERPA produces well-behaved real-emission contributions. As an illustration, we present the real-emission contributions—including dipole-subtraction terms—to the p_T distribution of the fourth jet, for a single subprocess with the maximum number of gluons.

1. Introduction

In the coming years a major theoretical task will be to provide reliable predictions for hard-scattering processes at the LHC. The start of the LHC era in particle physics opens new opportunities to confront data with theoretical predictions at scales well beyond those probed in previous colliders. The first observation at the LHC of W-boson production in association with jets marks an important milestone. Processes involving vector bosons are central to the physics program of the LHC. They are backgrounds to Higgs and top physics, as well as to many signals of new physics. Theoretical predictions can play an important role in experimentally-driven determinations of backgrounds, improving extrapolations to signal regions. Z and W production can play complementary roles in such determinations of backgrounds. At low luminosity, W production can be used to calibrate estimates of Z production, because its cross section is higher; while at high luminosity, Z production can be used to calibrate W production because of the cleanliness of measuring lepton pairs. The good theoretical understanding of vector-boson production also allows its use to measure the luminosity.

Next-to-leading-order (NLO) QCD is a key tool for confronting theory with experiment. This order in perturbation theory is the first to provide quantitatively reliable results, as it is the first order at which quantum corrections compensate the renormalization- and factorization-scale dependence in the strong coupling α_s. That scale dependence in leading-order (LO) predictions increases with the number of jets because of the increasing number of powers of α_s. At LO the scale dependence can be quite large, on the order of 50% for three or more jets. Furthermore, LO results may not model the shapes of distributions correctly. Although NLO computations are more challenging, in general they yield results with better reliability and agreement with measurements

*Presenter

Work supported in part by US Department of Energy contract DE-AC02-76SF00515.

(see *e.g.* refs. [1–9]).

For many years the bottleneck blocking NLO computations of vector-boson production with three or more jets has been the difficulty of evaluating the required one-loop amplitudes. The unitarity method [10,11], along with various important developments [12,13], has broken past this barrier, producing NLO results for vector-boson production in association with three jets [5, 8]. (See refs. [4,6] for other unitarity-based results, using various leading-color approximations to $W + 3$ jets at NLO.) NLO computations of six-point processes involving heavy quarks have also been carried out recently, using both Feynman diagrams and on-shell methods [9].

In this talk we briefly review the NLO results for $W, Z+3$-jet production presented in refs. [5,8]. We also present new results on Z boson production at the LHC, and demonstrate the feasibility of computing $W + 4$-jet production at NLO. The latter process is key for new physics searches at the LHC, and from a theoretical point of view goes one jet beyond the 2007 Les Houches "experimenters' wishlist" [1]. We show that the virtual matrix elements computed by the BlackHat library are numerically stable for the most complicated partonic subprocesses, those involving the maximum number of gluons. We also show that, after augmenting SHERPA with tree-level matrix elements from BlackHat and incorporating an updated integrator [14], we can obtain smooth distributions for the real-emission terms. As an illustration we present the infrared-subtracted real-emission contribution for a single subprocess.

2. Calculational Setup

NLO corrections to cross sections require the evaluation of virtual and real-emission contributions. We evaluate the virtual amplitudes using the BlackHat library [15,5], a numerical implementation of on-shell methods [10–13] at one loop. For the real emission contributions we use the Catani–Seymour dipole subtraction method [16], as implemented [17] in the program AMEGIC++ [18] (part of the SHERPA framework [19]) to cancel the infrared divergences arising in the phase-space integration. For subprocesses with up to eight external legs we use AMEGIC++ to generate any required tree amplitudes. We also use the SHERPA package to carry out the numerical integration over phase space. Details of the setup can be found in refs. [15,5,8].

3. Results for Vector-Boson Production with Three Jets

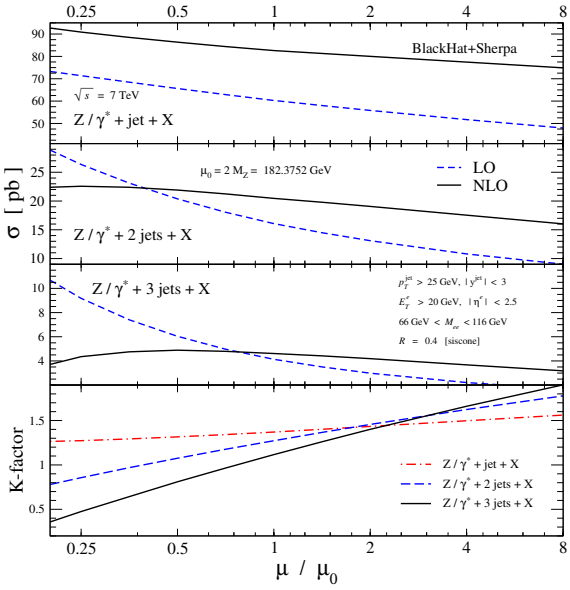

Figure 1. The scale dependence of the LO (dashed blue) and NLO (solid black) cross sections for $Z, \gamma^* + 1, 2, 3$-jet production at the LHC running at 7 TeV, as a function of the common renormalization and factorization scale μ, with $\mu_0 = M_Z$. The bottom panel shows the K factors, or ratio between the NLO and LO result, for each of the three cases: 1 jet (dot-dashed red), 2 jets (dashed blue), and 3 jets (solid black).

In ref. [5] we presented a detailed study of W + 3-jet production at NLO, at the Tevatron and LHC. This study exhibits the expected scale-dependence reduction, and correspondingly better theoretical precision, compared with earlier LO predictions. In addition, the study shows that

at the LHC, W^+ and W^- are *both* preferentially polarized left-handed at large transverse momentum. This effect is also present in $W + 1, 2$-jet production, and at LO as well. Such polarization will be largely, if not completely, absent in W bosons emerging from decays of top quarks or other new heavy states. Accordingly, it should be useful in setting experimental cuts that will distinguish between such daughter Ws and 'prompt' ones emitted directly in the short-distance process. In this Proceeding, we will discuss the more recent NLO computation of $Z + 3$-jet production at the Tevatron [8], for which data already exists [3,7], as well as new results for the current 7 TeV run of the LHC.

The renormalization- and factorization-scale dependence of NLO cross sections are greatly reduced with respect to LO, as illustrated in fig. 1 for $Z, \gamma^* + 1, 2, 3$-jet production at the LHC at 7 TeV. For these plots the SISCone jet algorithm [20] is used with cone size $R = 0.4$ and merging parameter $f = 0.75$; the lepton and jet cuts are indicated on the figure. (The case of three jets uses a leading-color approximation with the same separation of leading and subleading terms described in ref. [8]; we expect it to be accurate to within a few percent.) Indeed, the scale-dependence reduction becomes more pronounced as the number of jets increases, in accord with the increasing variation due to increasing powers of α_s in the LO calculation. The corresponding plot for Tevatron production [8] shows similar behavior.

In the left panel of fig. 2 we compare our NLO evaluation of p_T distributions [8] to D0 data for the third-jet p_T. D0 provided results for two data selections [7], with the Z decaying into and electron-positron pair. Fig. 2 uses the primary data selection based on the cuts, $p_T^{\rm jet} > 20$ GeV, $|\eta^{\rm jet}| < 2.5$, and 65 GeV $< M_{ee} <$ 115 GeV. D0 defined jets using the D0 Run II midpoint jet algorithm [21], with a cone size of $R = 0.5$ and a merging/splitting fraction of $f = 0.5$. Because this algorithm is not infrared-safe, we use instead the SISCone algorithm [20], with the same parameters, and a scale choice $\mu = \hat{H}_T/2$. In carrying out this comparison, we use the non-perturbative corrections estimated in ref. [7].

As can be seen from the figure the agreement between NLO theory and experiment is good despite a number of issues, including the difficulty of obtaining precise nonperturbative corrections, an extrapolation of measured data by DO using an LO-based program, and differences in the jet algorithms. Further details of comparisons to CDF and DO data for Z-boson production in association with jets may be found in ref. [8].

The right panel of fig. 2, shows the same distribution in 7 TeV collisions at the LHC. We again use the SISCone jet algorithm and a set of experimental cuts labeled on the plot. We note that NLO calculations for LHC data can use the same jet algorithms as the experiments, as the latter have adopted infrared-safe jet algorithms [22]. It should also be possible to minimize the effects of non-perturbative effects by choosing appropriate cone sizes [22], perhaps in a p_T-dependent fashion.

4. Towards $W + 4$ Jets

$W + 4$-jet production has been an important background since the early days of the Tevatron. There, it was the dominant background to $t\bar{t}$ production; at the LHC, it will be an important background to many new-physics searches, and will continue to be important to precision top-quark measurements. Its calculation beyond LO represents an important challenge to theorists. We report here on progress towards an NLO calculation of this process.

A crucial issue in the approach pursued in BlackHat is numerical stability of the virtual contributions. In fig. 3, we illustrate the stability of the leading-color virtual corrections to the squared matrix element, $d\sigma_V$, summed over colors and over all helicity configurations for the subprocesses $gd \to e^-\bar{\nu}gggu$. The horizontal axis of fig. 3 shows the logarithmic error,

$$\log_{10}\left(|d\sigma_V^{\rm BH} - d\sigma_V^{\rm target}|/|d\sigma_V^{\rm target}|\right),$$

for each of the three components: $1/\epsilon^2$, $1/\epsilon$ and ϵ^0, where $\epsilon = (4 - D)/2$ is the dimensional regularization parameter. In this expression $\sigma_V^{\rm BH}$ is the cross section computed by BlackHat as it

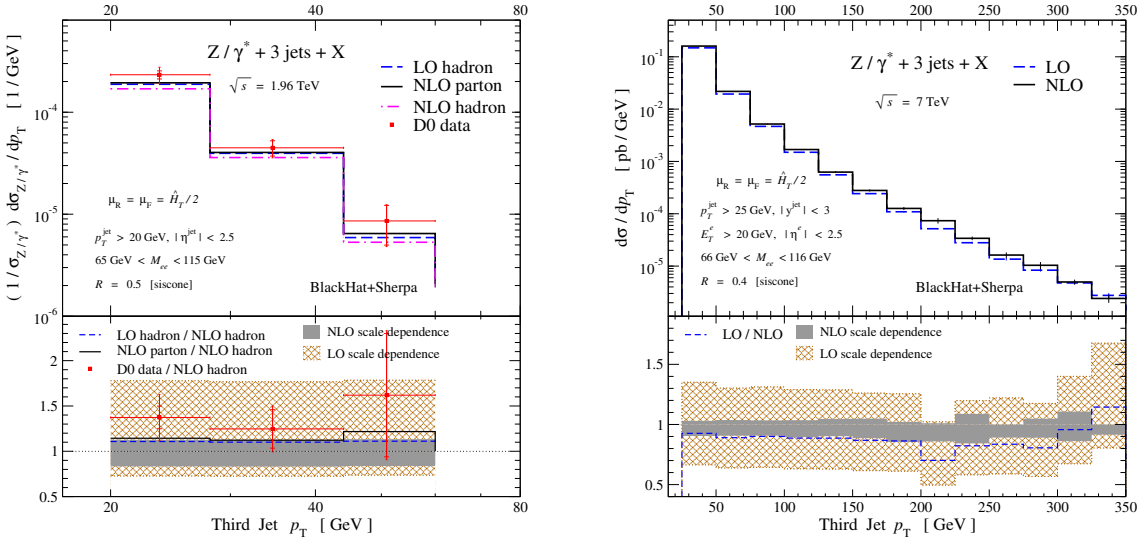

Figure 2. The left plot shows $1/\sigma_{Z,\gamma^*} \times d\sigma/dp_T$ at for the third-hardest jet in $Z, \gamma^* + 3$-jet production, comparing D0 data against LO and NLO predictions. In the upper panel the parton-level NLO distributions are the solid (black) histograms, while the NLO distributions corrected to hadron level are given by dash-dot (magenta) histograms. The D0 data is indicated by the (red) points. The LO predictions corrected to hadron level are shown as dashed (blue) lines. The lower panel shows the distribution normalized to the full hadron-level NLO prediction. The scale-dependence bands in the lower panels are shaded (gray) for NLO and cross-hatched (brown) for LO. The right plot shows the $d\sigma/dp_T$ distribution for the third-hardest jet at the LHC running at 7 TeV, with the indicated cuts. The complete color dependence is included in this plot, but no corrections to hadron level are included.

normally operates for production runs, whereas σ_V^{target} is a target value computed by BlackHat using higher-precision arithmetic of at least 32 digits. The phase-space points are selected in the same way as those used to compute cross sections. As seen in fig. 3, no point has a relative errors larger than about one part in 100; this level of precision is more than adequate for phenomenological studies.

What about the real corrections? In fig. 4 we show a p_T-distribution for the real-emission contributions, including dipole subtractions. Although these contributions are not physically meaningful by themselves (they need to be combined with dipole terms and the virtual corrections, and at the very least summed over other single-quark-line subprocesses), they do serve to illustrate that our SHERPA-based integration setup has them under control. In this calculation, we used the anti-k_t algorithm and took the center of mass energy to be 7 TeV. We applied a jet cut of $p_T > 25$ GeV, along with other cuts on the leptons and the rapidities of the jets. This plot is based on a calculation that used 2×10^8 phase-space points, yielding the rather small integration errors indicated by the thin vertical lines. Two key improvements in our setup which make the real contributions feasible are an improved integrator [14,8] and more efficient nine-point tree-level amplitudes generated by BlackHat using on-shell recursion relations [23].

5. Conclusion

A publicly available version of BlackHat is under construction and is being tested in a variety of projects (see *e.g.* ref. [24]). This version uses the Binoth Les Houches interface [25]. It has been tested with both C++ and Fortran clients. We intend the public version to provide all pro-

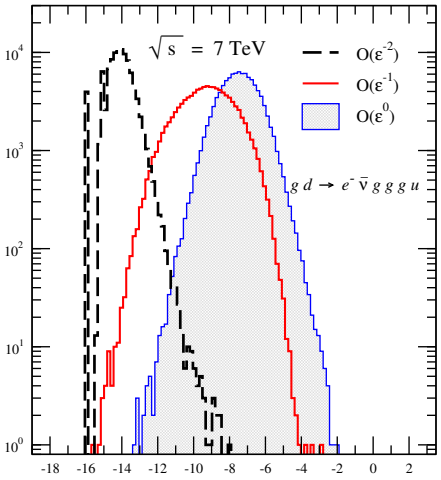

Figure 3. The distribution of the relative error in the leading-color virtual cross section for the subprocesses $gd \to e^-\bar{\nu}gggu$. The horizontal axis is the logarithm of the relative error between an evaluation by BlackHat, running in production mode, and a higher precision target. The vertical axis shows the number of phase-space points out of 100,000 that have the corresponding error. The dashed (black) line shows the $1/\epsilon^2$ term; the solid (red) curve, the $1/\epsilon$ term; and the shaded (blue) curve, the finite (ϵ^0) term.

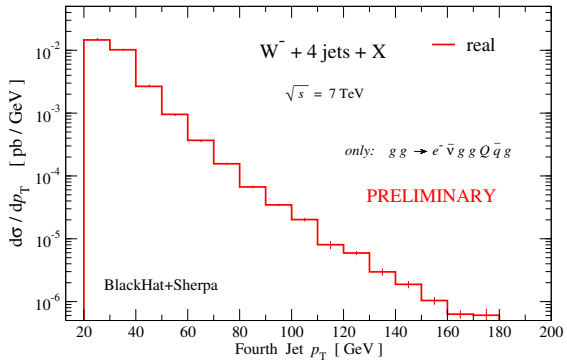

Figure 4. The real part of the NLO p_T distribution for the fourth jet in W + 4-jet production at the LHC. Only the subprocess $gg \to e^-\bar{\nu}ggQ\bar{q}g$ is included here. The thin vertical lines, where visible, indicate numerical integration uncertainties.

cesses that have been thoroughly vetted using the full BlackHat code. We expect significant further gains in efficiency after implementing a variety of additional optimizations, such as taking advantage of phase-space symmetries to reduce the amount of computation.

In summary, NLO calculations of V + 3-jet production (where V is a vector boson) at hadron colliders are under excellent control, using BlackHat and SHERPA. This has been confirmed in comparisons [4,8,5] to Tevatron data [2,3,7]. The frontier has now shifted to the long-awaited calculations of V + 4-jet production. In this Proceeding, we presented significant new progress towards this goal, and have demonstrated for a selected subprocess that the programs are able to carry out these complex calculations. After further optimizing and testing we plan to carry out NLO studies of V + 4-jet production at the LHC. More generally, we look forward to applying these tools to a wide range of studies of LHC physics.

Acknowledgments

This research was supported by the US Department of Energy under contracts DE–FG03–91ER40662, DE–AC02–76SF00515 and DE–FC02–94ER40818. DAK's research is supported by the European Research Council under Advanced Investigator Grant ERC–AdG–228301. HI's work is supported by a grant from the US LHC Theory Initiative through NSF contract PHY-0705682. This research used resources of Academic Technology Services at UCLA, PhenoGrid using the GridPP infrastructure, and the National Energy Research Scientific Computing Center, which is supported by the Office of Science of the U.S. Department of Energy under Contract No. DE–AC02–05CH11231.

REFERENCES

1. Z. Bern *et al.*, 0803.0494 [hep-ph]; T. Binoth *et al.*, 1003.1241 [hep-ph].
2. T. Aaltonen *et al.* [CDF], Phys. Rev. D **77**, 011108 (2008) [0711.4044 [hep-ex]].
3. T. Aaltonen *et al.* [CDF], Phys. Rev. Lett. **100**, 102001 (2008) [0711.3717 [hep-ex]].

4. C. F. Berger, Z. Bern, L. J. Dixon, F. Febres Cordero, D. Forde, T. Gleisberg, H. Ita, D. A. Kosower and D. Maître, Phys. Rev. Lett. **102**, 222001 (2009) [0902.2760 [hep-ph]].
5. C. F. Berger, Z. Bern, L. J. Dixon, F. Febres Cordero, D. Forde, T. Gleisberg, H. Ita, D. A. Kosower and D. Maître, Phys. Rev. D **80**, 074036 (2009) [0907.1984 [hep-ph]].
6. R. K. Ellis, K. Melnikov and G. Zanderighi, Phys. Rev. D **80**, 094002 (2009) [0906.1445 [hep-ph]]; K. Melnikov and G. Zanderighi, Phys. Rev. D **81**, 074025 (2010) [0910.3671 [hep-ph]].
7. V. M. Abazov *et al.* [D0], Phys. Lett. B **678**, 45 (2009) [0903.1748 [hep-ex]].
8. C. F. Berger, Z. Bern, L. J. Dixon, F. Febres Cordero, D. Forde, T. Gleisberg, H. Ita, D. A. Kosower and D. Maître, 1004.1659 [hep-ph].
9. A. Bredenstein, A. Denner, S. Dittmaier and S. Pozzorini, JHEP **0808**, 108 (2008) [0807.1248 [hep-ph]]; Phys. Rev. Lett. **103**, 012002 (2009) [0905.0110 [hep-ph]]; JHEP **1003**, 021 (2010) [1001.4006 [hep-ph]]; G. Bevilacqua, M. Czakon, C. G. Papadopoulos, R. Pittau and M. Worek, JHEP **0909**, 109 (2009) [0907.4723 [hep-ph]]; T. Binoth, N. Greiner, A. Guffanti, J. P. Guillet, T. Reiter and J. Reuter, Phys. Lett. B **685**, 293 (2010) [0910.4379 [hep-ph]]; G. Bevilacqua, M. Czakon, C. G. Papadopoulos and M. Worek, Phys. Rev. Lett. **104**, 162002 (2010) [1002.4009 [hep-ph]].
10. Z. Bern, L. J. Dixon, D. C. Dunbar and D. A. Kosower, Nucl. Phys. B **425**, 217 (1994) [hep-ph/9403226]; Nucl. Phys. B **435**, 59 (1995) [hep-ph/9409265]; Z. Bern, L. J. Dixon and D. A. Kosower, Ann. Rev. Nucl. Part. Sci. **46**, 109 (1996) [hep-ph/9602280].
11. Z. Bern, L. J. Dixon and D. A. Kosower, Annals Phys. **322**, 1587 (2007) [0704.2798 [hep-ph]]; C. F. Berger and D. Forde, 0912.3534 [hep-ph].
12. Z. Bern, L. J. Dixon and D. A. Kosower, Nucl. Phys. B **513**, 3 (1998) [hep-ph/9708239]; JHEP **0408**, 012 (2004) [hep-ph/0404293]; R. Britto, F. Cachazo and B. Feng, Nucl. Phys. B **725**, 275 (2005) [hep-th/0412103]; G. Ossola, C. G. Papadopoulos and R. Pittau, Nucl. Phys. B **763**, 147 (2007) [hep-ph/0609007]; W. T. Giele, Z. Kunszt and K. Melnikov, JHEP **0804**, 049 (2008) [0801.2237 [hep-ph]]; D. Forde, Phys. Rev. D **75**, 125019 (2007) [0704.1835 [hep-ph]]; S. D. Badger, JHEP **0901**, 049 (2009) [0806.4600 [hep-ph]].
13. C. F. Berger, Z. Bern, L. J. Dixon, D. Forde and D. A. Kosower, Phys. Rev. D **74**, 036009 (2006) [hep-ph/0604195].
14. A. van Hameren and C. G. Papadopoulos, Eur. Phys. J. C **25**, 563 (2002) [hep-ph/0204055]; T. Gleisberg, S. Höche and F. Krauss, 0808.3672 [hep-ph].
15. C. F. Berger, Z. Bern, L. J. Dixon, F. Febres Cordero, D. Forde, H. Ita, D. A. Kosower and D. Maître, Phys. Rev. D **78**, 036003 (2008) [0803.4180 [hep-ph]]; 0808.0941 [hep-ph].
16. S. Catani and M. H. Seymour, Phys. Lett. B **378**, 287 (1996) [hep-ph/9602277]; Nucl. Phys. B **485**, 291 (1997) [Erratum-ibid. B **510**, 503 (1998)] [hep-ph/9605323].
17. T. Gleisberg and F. Krauss, Eur. Phys. J. C **53**, 501 (2008) [0709.2881 [hep-ph]].
18. F. Krauss, R. Kuhn and G. Soff, JHEP **0202**, 044 (2002) [hep-ph/0109036].
19. T. Gleisberg, S. Höche, F. Krauss, M. Schönherr, S. Schumann, F. Siegert and J. Winter, JHEP **0902**, 007 (2009) [0811.4622 [hep-ph]].
20. G. P. Salam and G. Soyez, JHEP **0705**, 086 (2007) [0704.0292 [hep-ph]].
21. G.C. Blazey, *et al.*, in *Proceedings of the Workshop: QCD and Weak Boson Physics in Run II*, Fermilab-Pub-00/297 (2000).
22. G. P. Salam, 0906.1833 [hep-ph].
23. R. Britto, F. Cachazo, B. Feng and E. Witten, Phys. Rev. Lett. **94**, 181602 (2005) [hep-th/0501052].
24. R. Frederix, in *Proceedings of RADCOR 2009*, PoS **RADCOR2009**, 066 (2009).
25. T. Binoth *et al.*, 1001.1307 [hep-ph].